Journal of Physics G: Nuclear and Particle Physics

PAPER

Prediction of $h \to \gamma Z$ from $h \to \gamma\gamma$ at the LHC for the IMDS$_3$ model

To cite this article: E C F S Fortes *et al* 2015 *J. Phys. G: Nucl. Part. Phys.* **42** 115001

IOP Publishing Journal of Physics G: Nuclear and Particle Physics

J. Phys. G: Nucl. Part. Phys. **42** (2015) 115001 (17pp) doi:10.1088/0954-3899/42/11/115001

Prediction of $h \to \gamma Z$ from $h \to \gamma\gamma$ at the LHC for the IMDS$_3$ model

E C F S Fortes, A C B Machado, J Montaño[1] and V Pleitez

Instituto de Física Teórica–Universidade Estadual Paulista R. Dr Bento Teobaldo Ferraz 271, Barra Funda São Paulo—SP, 01140-070, Brazil

E-mail: elaine@ift.unesp.br, ana@ift.unesp.br, montano@ift.unesp.br and vicente@ift.unesp.br

Received 12 May 2015, revised 13 August 2015
Accepted for publication 17 August 2015
Published 24 September 2015

Abstract

We consider the decays $h \to \gamma\gamma$, γZ in the context of an extension of the Standard Model with two inert doublets and an additional S_3 symmetry. This model contributes to for these processes through new charged scalar-loops. Comparing our $h \to \gamma\gamma$ with more precise available experimental data we can predict the behavior of $h \to \gamma Z$ since they depend on the same parameters. Our estimation for this channel is 1.05 times the standard model value, but it can be as high as 1.16 if we consider the $+1\sigma$ uncertainty from the $h \to \gamma\gamma$ data, and as low as 0.96 if we consider -1σ.

Keywords: particle physics, Higgs physics, radiative corrections

(Some figures may appear in colour only in the online journal)

1. Introduction

The Large Hadron Collider (LHC) results indicate, for the first time, that at least one fundamental neutral scalar, here denoted by h, exists in nature. Moreover, all its properties that have been measured so far are compatible with the predictions of the Standard Model (SM), the Higgs boson. For instance, it is a spin-0 and charge conjugation and party symmetry even scalar [1, 2] and its couplings with gauge bosons and heavy fermions are compatible with those of the SM within the experimental error [3, 4]. Notwithstanding, the data do not rule out the existence of new physics; in particular, processes induced at loop level have always been important when seeking such evidence. This is the case of the decays $h \to \gamma\gamma$ and $h \to \gamma Z$ because they may have contributions from new charged particles. Recently, ATLAS and CMS Collaborations have measured the decay ratios for both processes [5–8]. The decay of

[1] Author to whom any correspondence should be addressed.

Table 1. Ratios of the experimental measured values compared to the SM predictions reported by ATLAS and CMS. In this work we use the CMS data for the two photons process because it gives the more stringent deviation.

Ratio	ATLAS	CMS
$R_{\gamma\gamma}$	$1.17^{+0.27}_{-0.27}$ [5]	$1.14^{+0.26}_{-0.23}$ [6]
$R_{\gamma Z}$	<11 [7]	<9.5 [8]

the Higgs boson into two photons is now in agreement with the SM prediction, if compared to 2012 data, but the decay into a photon and a Z has not been observed yet; however, ATLAS and CMS have presented upper limits for this decay (see table 1).

Moreover, motivated by physics of the dark matter (DM), neutrinos masses, hierarchy problems, and any other physics beyond the SM, there are many phenomenological models that extend the scalar sector of the SM with one or more scalar multiplets. In fact, if in the future it becomes clear that DM consists of several components, multi-Higgs models will be natural candidates. In particular n-doublet models with $n \geqslant 2$, with or without scalar singlets and triplets, will be interesting possibilities. In particular, the inert Higgs doublet model (IDM) is the simplest model incorporating two DM candidates: one scalar and one pseudo-scalar field. A two inert doublet model can be obtained from a 3HDM plus a Z_2 symmetry with the inert doublets being odd and all the other fields even under Z_2. Because of this symmetry, the two inert doublets do not get a vacuum expectation value (VEV), but the scalar potential is as complicated as the general three Higgs doublet model (3HDM). The two inert doublets interact with each other as in the case of a general two Higgs doublet model (2HDM): i.e., 10 real dimensionless coupling constants, λs. Moreover, each inert doublet interacts with the SM-like Higgs doublet as a 2HDM+Z_2 model, i.e., 10 λs more. It means that a two inert doublet model with just a Z_2 symmetry implies 23 real dimensionless parameters. A more economical 3HDM with two doublets being inert can be built by imposing an S_3 symmetry. The S_3 symmetry allows the symmetry eigenstates to be related to the mass eigenstates through a tri-bimaximal-like matrix, i.e., the mixing angles in all the scalar sectors are the same and of the Clebsch-Gordan coefficients type, and there are no arbitrary mixing angles in the scalar sectors. This is not the case in the general 3HDM with an arbitrary vacuum alignment. This sort of model was put forward for the first time in [9] and the $h \to \gamma\gamma$ branching ratio in this context was considered in [10]. Here we will revisit this process with the more recent experimental data and also include the $h \to \gamma Z$ process. We call this model IDMS_3 as in [11], where we have shown that the model has DM candidates. The Higgs mechanism provides a portal for communication between the inert sector and the known particles.

In the IDM and 3HDMS_3 the production of the 125 GeV Higgs is the same as in the SM; however, the decays $h \to \gamma\gamma$ and $h \to \gamma Z$ can receive corrections due to the contributions of charged scalars in loops. The phenomenology of IDM has been extensively discussed: i) in the context of DM phenomenology [12–17], ii) for collider phenomenology [18–20] and, iii) IDM has also been advocated to improve the naturalness idea [21–23]. However, all these references were published before the LHC data. The ratios of $h \to \gamma\gamma$ and $h \to \gamma Z$ were analyzed in the context of a general 3HDM in [24]. However, these authors do not consider the case of two inert doublets and, unlike the present model, their model has arbitrary mixing matrices in the scalar sectors.

Special attention requires the $h \to \gamma Z$ rare decay since the current first attempt at measuring this channel at LHC Run 1 shed an upper limit of one order of magnitude with

respect to the SM prediction ($R_{\gamma Z} = 1$)—see table 1. This is because the available luminosity at LHC is not sensitive enough to collect sufficient data for this process. Specifically, ATLAS [7] has reported an upper limit of 11 times the SM expectation, using a luminosity of 4.5 fb^{-1} of pp collisions at $\sqrt{s} = 7$ TeV and 20.3 fb^{-1} at $\sqrt{s} = 8$ TeV; CMS [8] reported an upper limit of 9.5 times the SM prediction, with integrated luminosities of 5.0 fb^{-1} and 19.6 fb^{-1} at pp collisions of 7 TeV and 8 TeV, respectively. Nevertheless, the future of the detection of $h \to \gamma Z$ seems a difficult task according to the future LHC upgrades schedule [25, 26]: at LHC Run 3 with 14 TeV will allow the collection of 300 fb^{-1} of data where the precision on the signal strength is expected to be 145%–147% at ATLAS and 54%–57% at CMS, and at Run 6 with 3000 fb^{-1} the precision is expected to be 62% at ATLAS and 20%–24% at CMS. Therefore, an accurate value for this decay will be one of the last data obtained by the LHC, but it is possible to predict the behavior of this decay from the process $h \to \gamma\gamma$ in the IDMS_3 due to the correlation of their common parameters; specifically, we estimate that considering up to $\pm 1\sigma$ deviation from the experimental $R_{\gamma\gamma}$ data, there is no possiblity of a positive deviation larger than 1.16 times the SM value, nor a suppression beyond 0.96.

The outline of this paper is as follows. In section 2 we briefly present the model of [9]. In section 3 we calculate the decays $h \to \gamma\gamma$, γZ in terms of the respective widths in the SM. The last section gives our conclusions. In the appendix we present the amplitudes of the two processes and also details about the form factors and their solutions in terms of the Passarino–Veltman scalar functions and their analytical solutions.

2. The model

In [9] an extension of the electroweak standard model with three Higgs scalars was presented, all of them transforming as doublets under $SU(2)$ and having $Y = +1$. Some fields transform under S_3 as a doublet $D \equiv \mathbf{2}$, and some as a singlet $S \equiv \mathbf{1}$. The scalar transform under S_3 as

$$\begin{aligned} S &= \frac{1}{\sqrt{3}}\left(H_1 + H_2 + H_3\right) \sim \mathbf{1}, \\ D \equiv \left(D_1, D_2\right) &= \left[\frac{1}{\sqrt{6}}\left(2H_1 - H_2 - H_3\right), \frac{1}{\sqrt{2}}\left(H_2 - H_3\right)\right] \sim \mathbf{2}. \end{aligned} \tag{1}$$

The vacuum alignment is given by $\langle H_1 \rangle = \sqrt{3}\, v_{\rm SM}$, and $\langle H_2, H_3 \rangle = 0$ is a stable minimum of the potential, at least at the tree level.

The most general scalar potential invariant under $SU(2) \otimes U(1)_Y \otimes S_3$ symmetry is given by:

$$\begin{aligned} V(D, S) = {} & \mu_s^2 S^\dagger S + \mu_d^2\left[D^\dagger \otimes D\right]_{\mathbf{1}} + \lambda_1\left(\left[D^\dagger \otimes D\right]_{\mathbf{1}}\right)^2 + \lambda_2\left[\left(D^\dagger \otimes D\right)_{\mathbf{1}'}\left(D^\dagger \otimes D\right)_{\mathbf{1}'}\right] \\ & + \lambda_3\left[\left(D^\dagger \otimes D\right)_{\mathbf{2}'}\left(D^\dagger \otimes D\right)_{\mathbf{2}'}\right]_{\mathbf{1}} + \lambda_4\left(S^\dagger S\right)^2 \\ & + \lambda_5\left[D^\dagger \otimes D\right]_{\mathbf{1}} S^\dagger S + \left[\lambda_6\left[\left[S^\dagger D\right]_{\mathbf{2}'}\left[S^\dagger D\right]_{\mathbf{2}'}\right]_{\mathbf{1}}\right. \\ & \left. + H.\,c.\right] + \lambda_7 S^\dagger\left[D \otimes D^\dagger\right]_{\mathbf{1}} S + \left[\lambda_8\left[\left(S^\dagger \otimes D\right)_{\mathbf{2}'}\left(D^\dagger \otimes D\right)_{\mathbf{2}'}\right]_{\mathbf{1}} + H.\,c.\right] \end{aligned} \tag{2}$$

Denoting an arbitrary doublet by $\mathbf{2} = (x_1, x_2)$, we have the product rule **S** as $\mathbf{2} \otimes \mathbf{2} = \mathbf{1} \oplus \mathbf{1}' \oplus \mathbf{2}'$ where $\mathbf{1} = x_1 y_1 + x_2 y_2$, $\mathbf{1}' = x_1 y_2 - x_2 y_1$, $\mathbf{2}' = (x_1 y_2 + x_2 y_1, x_1 y_1 - x_2 y_2)$, and $\mathbf{1}' \otimes \mathbf{1}' = \mathbf{1}$ [27]. Let us define $S = (s^+\ s^0)^T$, $D_i = (d_i^+\ d_i^0)^T$, $i = 1, 2$. In terms of the S and

D_i fields, the potential in equation (2) is written as

$$\begin{aligned} V(S, D_1, D_2) = {} & \mu_s^2 S^\dagger S + \mu_d^2\left(D_1^\dagger D_1 + D_2^\dagger D_2\right) \\ & + \lambda_1\left(D_1^\dagger D_1 + D_2^\dagger D_2\right)^2 + \lambda_2\left(D_1^\dagger D_2 - D_2^\dagger D_1\right)^2 \\ & + \lambda_3\Big[\left(D_1^\dagger D_2 + D_2^\dagger D_1\right)^2 + \left(D_1^\dagger D_1 - D_2^\dagger D_2\right)^2\Big] \\ & + \lambda_4\left(S^\dagger S\right)^2 + \lambda_5\left(D_1^\dagger D_1 + D_2^\dagger D_2\right)S^\dagger S \\ & + \Big[\lambda_6\left(S^\dagger D_1 S^\dagger D_1 + S^\dagger D_2 S^\dagger D_2\right) + H.\,c.\Big] + \lambda_7 S^\dagger\left(D_1 D_1^\dagger + D_2 D_2^\dagger\right)S \\ & + \lambda_8\Big[S^\dagger D_1\left(D_1^\dagger D_2 + D_2^\dagger D_1\right) + S^\dagger D_2\left(D_1^\dagger D_1 - D_2^\dagger D_2\right) + H.\,c.\Big] \end{aligned} \tag{3}$$

If $\mu_d^2 > 0$, only the singlet S gains a VEV; and if $\lambda_8 = 0$, this vacuum is stable at tree and the one-loop level. For this term to be forbidden, we impose a Z_2 symmetry under which $D \to -D$, and S and all the other fields are even. The decomposition of the symmetry eigenstates we make as usual, as $H_i^0 = (1/\sqrt{2})(v_i + \eta_i^0 + i\, a_i^0)$, $i = 1, 2, 3$. We assume for the sake of simplicity that the VEVs are real and also equal, i.e., $v_1 = v_2 = v_3 = v$. these constraint equations are reduced to a simple equation:

$$t_1 = t_2 = t_3 = v\left(\mu_s^2 + 3\lambda_4 v^2\right), \tag{4}$$

and if $t_i = 0$, we have $\mu_s^2 = -3\lambda_4 v^2 = -\lambda_4 v_{\rm SM}^2 < 0$, which implies that $\lambda_4 > 0$.

The masses are given by:

$$\begin{aligned} & m_h^2 = 2\lambda_4 v_{\rm SM}^2, && m_{h_2}^2 = m_{h_3}^2 \equiv m_H^2 = \mu_d^2 + \frac{1}{2}\lambda' v_{\rm SM}^2, \\ & m_{A_1}^2 = 0, && m_{A_2}^2 = m_{A_3}^2 \equiv m_A^2 = \mu_d^2 + \frac{1}{2}\lambda'' v_{\rm SM}^2. \\ & m_{h^+}^2 = 0, && m_{h_2^+}^2 = m_{h_3^+}^2 \equiv m_{h^+}^2 = \frac{1}{4}\left(2\mu_d^2 + \lambda_5 v_{\rm SM}^2\right). \end{aligned} \tag{5}$$

Note that μ_d^2 is not related to the spontaneous symmetry breaking and since it is not protected by any symmetry, it may be larger than the electroweak scale. As we see in equation (5), h^+ and A^0 are the would-be Goldstone bosons, that give masses to the $W^\pm$ and Z gauge bosons and $h_{2,3}^0$ and $A_{2,3}^0$ are the inert fields. Due to the S_3 symmetry and the vacuum alignment, we have a residual symmetry and as a result, the mass eigenstates of the inert doublets are degenerate, as we can see in equation (5).

However, the residual symmetry can be broken with soft terms in the scalar potential. So, adding the following quadratic terms $\nu_{nm}^2 H_n^\dagger H_m$, $n, m = 2, 3$ and imposing that $\nu_{22}^2 = \nu_{33}^2 = -\nu_{23}^2 \equiv \nu^2$, the mass matrix will remain diagonalized by the matrix, so the inert character is maintained. The eigenvalues are now:

$$\begin{aligned} & \bar{m}_h^2 = m_h^2, \quad \bar{m}_{h_2}^2 = m_H^2, \quad \bar{m}_{h_3}^2 = m_H^2 + \nu^2, \\ & \bar{m}_{A_1}^2 = 0, \quad \bar{m}_{A2}^2 = m_A^2, \quad \bar{m}_{A3}^2 = m_A^2 + \nu^2, \\ & \bar{m}_{h_1^+}^2 = 0, \quad \bar{m}_{h_2^+}^2 = m_{h^+}^2, \quad \bar{m}_{h_3^+}^2 = m_{h^+}^2 + \nu^2, \end{aligned} \tag{6}$$

where m_h^2, m_A^2, $m_{h^+}^2$ and m_H^2 are given in equation (5).

The constraints from the vacuum stability as well as positivity on the relations of the couplings are as follows:

$$\begin{aligned}
&\lambda_4 > 0,\\
&\lambda_1 + \lambda_3 > 0,\\
&\lambda_5 + 2\sqrt{\lambda_4\left(\lambda_1 + \lambda_3\right)} > 0,\\
&\lambda_5 + \lambda_7 - 2\lambda_6 + 2\sqrt{\lambda_4\left(\lambda_1 + \lambda_3\right)} > 0,\\
&\lambda_1 + \lambda_3 > 4\lambda_2.
\end{aligned} \tag{7}$$

In the lepton and quark sectors all fields transform as singlets under S_3, implying that they only interact with the singlet S as follows:

$$-\mathcal{L}_{\text{Yukawa}} = \bar{L}_{iL}\left(G^{l}_{ij} l_{jR} S + G^{\nu}_{ij} \nu_{jR} \tilde{S}\right) + \bar{Q}_{iL}\left(G^{u}_{ij} u_{jR} \tilde{S} + G^{d}_{ij} d_{jR} S\right) + H.\,c.\,, \tag{8}$$

$\tilde{S} = i\tau_2 S^*$ and we have included right-handed neutrinos. For more details see [9].

The new inert scalar interactions with the gauge bosons, which arise from $(D_\mu h_i)^\dagger (D^\mu h_i)$ with $i = 2, 3$, in the physical basis ($h_i = (h_i^+, h_i^0)^T$) are given by

$$\begin{aligned}
\mathcal{L}_{\text{Gauge}} = {} & igs_W\left(\partial_\mu h_i^- h_i^+ - \partial_\mu h_i^+ h_i^-\right)A^\mu + igc_W\left(\frac{1 - t_W^2}{2}\right)\left(\partial_\mu h_i^- h_i^+ - \partial_\mu h_i^+ h_i^-\right)Z^\mu\\
& + i\frac{g}{\sqrt{2}}\left(\partial_\mu h_i^- h_i^0 - \partial_\mu h_i^0 h_i^-\right)W^{+\mu} - i\frac{g}{\sqrt{2}}\left(\partial_\mu h_i^+ h_i^0 - \partial_\mu h_i^0 h_i^+\right)W^{-\mu}\\
& + g^2\, s_W^2\, h_i^- h_i^+ A_\mu A^\mu + g^2 c_W^2\left(\frac{1 - t_W^2}{2}\right)^2\\
& \times h_i^- h_i^+ Z_\mu Z^\mu + 2g^2\, s_W c_W\left(\frac{1 - t_W^2}{2}\right)h_i^- h_i^+ A_\mu Z^\mu\\
& + \frac{g^2\, s_W}{2}\left(h_i^- W_\mu^+ + h_i^+ W_\mu^-\right)h_i^0 A^\mu + \frac{g^2 c_W}{2}\left(\frac{1 - t_W^2}{2}\right)\left(h_i^- W_\mu^+ + h_i^+ W_\mu^-\right)h_i^0 Z^\mu.
\end{aligned} \tag{9}$$

The interactions between scalars in the physical basis are obtained from the following Lagrangian

$$\begin{aligned}
\mathcal{L}_{\text{Scalars}} = {} & -\lambda_4 v_{\text{SM}} h^3 - \frac{\lambda_5 v_{\text{SM}}}{2}\left(h_2^- h_2^+ + h_3^- h_3^+\right)h - \frac{\lambda' v_{\text{SM}}}{2}h\left[\left(h_2^0\right)^2 + \left(h_3^0\right)^2\right] - \frac{\lambda_4}{4}h^4\\
& - \frac{\lambda'}{2}h^2\left[\left(h_2^0\right)^2 + \left(h_3^0\right)^2\right] - 2\lambda_3 h_2^0 h_3^0 h_2^- h_3^+ - \left(\lambda_1 + \lambda_3\right)\left(h_3^0\right)^2 h_3^- h_3^+\\
& - \left(\lambda_2 + \lambda_3\right)\left(h_2^- h_3^+\right)^2 - \left(\lambda_1 + \lambda_3\right)\left(h_2^- h_2^+\right)^2 - \frac{\lambda_1 + \lambda_3}{4}\left[\left(h_2^0\right)^4 + \left(h_3^0\right)^4\right]\\
& - \left(\lambda_1 + \lambda_3\right)\left(h_2^0\right)^2\left(h_2^- h_2^+ + h_3^- h_3^+\right),
\end{aligned} \tag{10}$$

where in particular the terms proportional to λ_5 are the couplings between the SM-Higgs with the charged scalars involved in the $h \to \gamma\gamma$, γZ decays.

3. Ratios $R_{\gamma\gamma}$ and $R_{\gamma Z}$

In this section we are going to study the ratios $R_{\gamma\gamma}$ and $R_{\gamma Z}$ predicted by the IDMS_3 with respect to the SM.

To explore the sensitivity of the processes $h \to \gamma\gamma$, γZ due to new spin-0 content in the IDMS_3 we have used the experimental data reported by ATLAS and CMS collaborations. As

can be seen in table 1, $h \to \gamma\gamma$ is within 1σ of the SM prediction, but for $h \to \gamma Z$ there is barely an upper limit of one order of magnitude above the SM prediction. For the Higgs decay into two photons see the experimental [5, 6], and for a photon and a Z [7, 8].

The S_3 symmetry and the vacuum alignment guarantee that the DM candidate does not decay into vector gauge bosons ($h_2^0 \to \gamma\gamma$, γZ) through quantum fluctuations induced by new charged spin-0 content, because the existence of the couplings $h_2^0 h_2^+ h_2^-$ and $h_2^0 h_3^+ h_3^-$, is forbidden; see equation (10), in contrast, as it occurs with the SM-Higgs h due to the presence of the couplings $h h_2^+ h_2^-$ and $h h_3^+ h_3^-$ that are proportional to λ_5.

It is known that the Higgs discovery channel is $pp \to gg \to h \to \gamma\gamma$, and because of the nature of the IDMS_3 the SM interactions between the Higgs and quarks remain intact; thus there are no novelties in the Higgs fabric side $pp \to gg \to h$. On the other hand, new physics effects could come from new spin-0 particles in the Higgs decay process. More specifically, because the cross section for the Higgs production $pp \to gg \to h$ is the same for the SM and the IDMS_3, the application of the narrow width approximation (NWA) at the resonant point (when the gluon fusion energy is $\sqrt{\hat{s}} = m_h$), allows us to analyze the ratio signals with pure on-shell information

$$\begin{aligned} R_{\gamma V} &\equiv \frac{\sigma(pp \to gg \to h \to \gamma V)^{\mathrm{IDM}S_3}}{\sigma(pp \to gg \to h \to \gamma V)^{\mathrm{SM}}} \\ &\overset{\mathrm{NWA}}{\simeq} \frac{\sigma(gg \to h)^{\mathrm{IDM}S_3}\mathrm{Br}(h \to \gamma V)^{\mathrm{IDM}S_3}}{\sigma(gg \to h)^{\mathrm{SM}}\mathrm{Br}(h \to \gamma V)^{\mathrm{SM}}} \\ &= \frac{\Gamma(h \to \gamma V)^{\mathrm{IDM}S_3}}{\Gamma(h \to \gamma V)^{\mathrm{SM}}} \frac{\Gamma_h^{\mathrm{SM}}}{\Gamma_h^{\mathrm{IDM}S_3}}, \end{aligned} \tag{11}$$

where $V \equiv \gamma, Z$. We would like to draw attention to the fact that in our scenarios the new neutral scalar masses forbid invisible decays of the SM-Higgs, except in the scenario 1a of table 1 of [11] in which the Born level yields $\Gamma(h \to h_3^0 h_3^0) \sim 10^{-6}\,\mathrm{GeV}$, which is highly suppressed and does not disturb the total Higgs width, hence $\Gamma_h^{\mathrm{IDM}S_3} \simeq \Gamma_h^{\mathrm{SM}}$, leading to

$$R_{\gamma V} = \frac{\Gamma(h \to \gamma V)^{\mathrm{IDM}S_3}}{\Gamma(h \to \gamma V)^{\mathrm{SM}}}. \tag{12}$$

As we have seen, the IDMS_3 gives rise to couplings between the new charged scalars and the SM-Higgs boson, and also with vector gauge bosons, but there are no modifications to the existing SM couplings, therefore for the decays $h \to \gamma\gamma$, γZ only a new scalar contribution is added to the existing ones.

The participating diagrams in the processes $h \to \gamma\gamma$, γZ are illustrated in figure 1 in the unitary gauge, where (a) corresponds to fermions, (b) and (c) to W gauge boson, and (d) and (e) to new charged scalars. We have constructed each diagram and performed the loop integrals with the Passarino–Veltman reduction method [28] using the package `FeynCalc` [29] which provides the results in terms of the scalar functions B_0 and C_0 [30]. We have also calculated their corresponding general analytical solutions, which lead to the known standard notations of [31–33]. Particularly here we work with the Djouadi notation [32, 33] for the width decays. In the appendix we report the amplitudes of the processes and give details of the correspondence between our direct results in terms of the B_0 and C_0 functions and the Djouadi notation.

In the following we present the decay widths showing explicitly only the new spin-0 contribution of the model. The other known spin-1/2 and spin-1 contributions are given in the appendix.

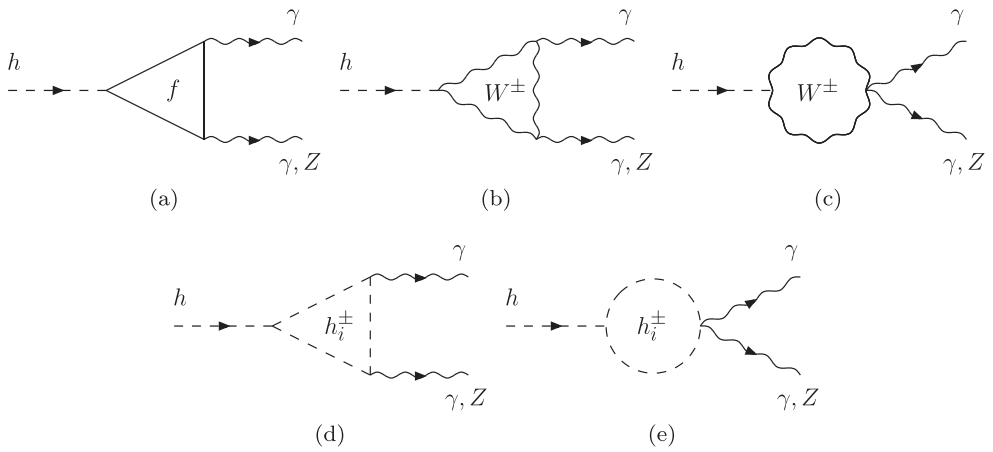

Figure 1. Decays $h \to \gamma\gamma$, γZ.

The Higgs decay into two photons has a new spin-0 contribution given by

$$\Gamma(h \to \gamma\gamma) = \frac{G_F \alpha^2 m_h^3}{128\sqrt{2}\pi^3} \left| \sum_{i=1}^{9} N_C^{f_i} Q_{f_i}^2 A_{1/2}^{\gamma\gamma}(\tau_{f_i}) + A_1^{\gamma\gamma}(\tau_W) + \frac{\lambda_5 v_{\rm SM}^2}{2} \sum_{i=2}^{3} \frac{1}{m_{h_i^+}^2} A_0^{\gamma\gamma}(\tau_{h_i^+}) \right|^2, \tag{13}$$

with the form factors $A_{\rm Spin}^{\gamma\gamma}$, where the charged scalar form factor is

$$A_0^{\gamma\gamma} \equiv -\left[\tau_{h^+} - f(\tau_{h^+})\right]\tau_{h^+}^{-2}. \tag{14}$$

The $f(\tau)$ function is presented in the appendix.

The Higgs decay into a photon and a Z also has a spin-0 contribution

$$\Gamma(h \to \gamma Z) = \frac{G_F^2 m_W^2 \alpha m_h^3}{64\pi^4}\left(1 - \frac{m_Z^2}{m_h^2}\right)^3 \left| \frac{2}{c_W} \sum_{i=1}^{9} N_C^{f_i} Q_{f_i} g_V^{f_i} A_{1/2}^{\gamma Z}(\tau_{f_i}) + A_1^{\gamma Z}(\tau_W) + \frac{\lambda_5 v_{\rm SM}^2 v_{h^\pm}}{2} \sum_{i=2}^{3} \frac{1}{m_{h_i^+}^2} A_0^{\gamma Z}(\tau_{h_i^+}) \right|^2, \tag{15}$$

where $v_{h^\pm} \equiv c_W(1 - t_W^2)$, $A_{\rm Spin}^{\gamma Z}$ are the form factors, with the new charged scalar contribution

$$A_0^{\gamma Z} \equiv -I_1. \tag{16}$$

See the appendix for detailed information about all the form factors, the $I_{1,2}$ auxiliary definitions and also the $f(\tau)$ and $g(\tau)$ functions and their relations with the Passarino–Veltman scalar functions.

In the next section we report our phenomenological analysis for $h \to \gamma\gamma$, γZ. We use the values $m_h = 125.09$ GeV with the more recent data from PDG Live: $m_W = 80.385$, $m_Z = 91.1876$, $m_u = 0.0023$, $m_d = 0.0048$, $m_s = 0.095$, $m_c = 1.275$, $m_b = 4.18$, $m_t = 173.07$, $m_e = 0.000511$, $m_\mu = 0.105658$, $m_\tau = 1.77682$; all values in GeV, $G_F = 1.1663787 \times 10^{-5}$ GeV^{-2}.

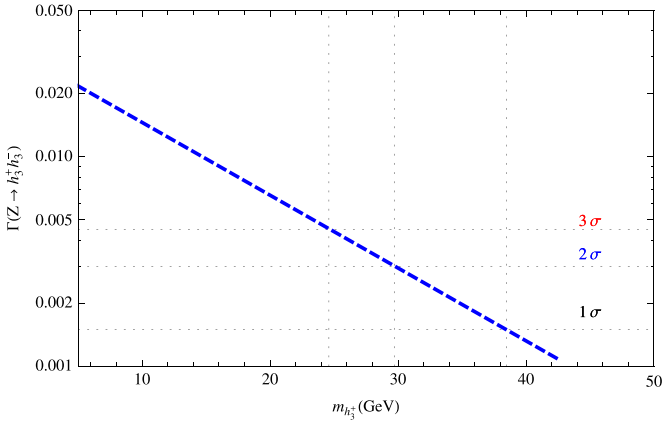

Figure 2. Z invisible decay width, as a function of the charged scalar h_3^+ mass. Imposing the error of the current value for the invisible decay as the allowed limit for the decay width, we a obtain a lower limit for the charged mass of 25 GeV.

The four collaborations of LEP [35] and ATLAS [36] have searched for charged scalars; notwithstanding, their lower limits depend on the model which is always the 2HDM. In LEP experiments, the searches include 2HDM of type I and II. Type I is searched in the ATLAS experiment. Both searches depend on the assumes branching ratio of the charged Higgs boson decays. ATLAS, for instance, assumes $H^+ \to c\bar{s} = 100\%$. Summarizing, ATLAS has observed no signal for H^+ masses between 90 GeV and 150 GeV, and LEP has excluded this sort of scalars with mass below 72.5 GeV for type I scenario and 80 GeV for type II scenario. However, none of these results apply to our model since the charged scalar, are inert and do not couple to fermions. Anyway, we will use 80 GeV for the mass of h_2^+ which is in the range of LEP and ATLAS results. For the other charged scalar, h_3^+ we will obtain a lower limit for its mass using its contribution to the Z boson invisible decay width, where we have found $m_{h_3^+} > 25$ GeV, if we consider a 3σ deviation for the invisible decay width in our calculations. These results can be appreciated in figure 2.

We first report the $h \to \gamma\gamma$ channel, and for the experimental comparison we use the data provided by the ATLAS [5] and CMS [6] collaborations, given in table 1. Specifically, we follow the more stringent data that is reported by CMS; we explore its deviations values until $\pm 3\sigma$.

In figure 3 we present $R_{\gamma\gamma}$ with $m_{h_2^+} = 80$ GeV. First, we show $R_{\gamma\gamma}$ as a function of $m_{h_3^+}$; in figure 3(a) we consider λ_5 negative and in figure 3(b) it is positive; in figure 3(c) $R_{\gamma\gamma}$ is presented as a function of $-0.6 \leqslant \lambda_5 \leqslant 0.6$, and different values of $m_{h_3^+}$ are chosen. From the three plots it can be appreciated that negative values of λ_5 and $m_{h_3^+} > m_h/2$ favor a positive deviation, being more compatible with the experimental allowed region if $m_{h_3^+} > 80$ GeV. For positive values of λ_5 and $m_{h_3^+} < m_h/2$ there is also a compatible positive deviation, but this mass scenario for the charged scalars could not be valid if the experimental values for one charged scalar mass limit from LEP [35] and ATLAS [36] are also valid for an extra charged scalar h_3^+. If future experimental data confirm a small negative deviation for $R_{\gamma\gamma}$, the S_3 model still has room for consistency with a scenario of positive λ_5 and $m_{h_{2,3}^+} > 80$ GeV.

Considering now $R_{\gamma Z}$, we have also made an analysis entirely analogous to the two photons case. The available experimental data for the process $h \to \gamma Z$ is still very rough; the ATLAS [7] and CMS [8] reports so far provide upper limits of one order of magnitude larger

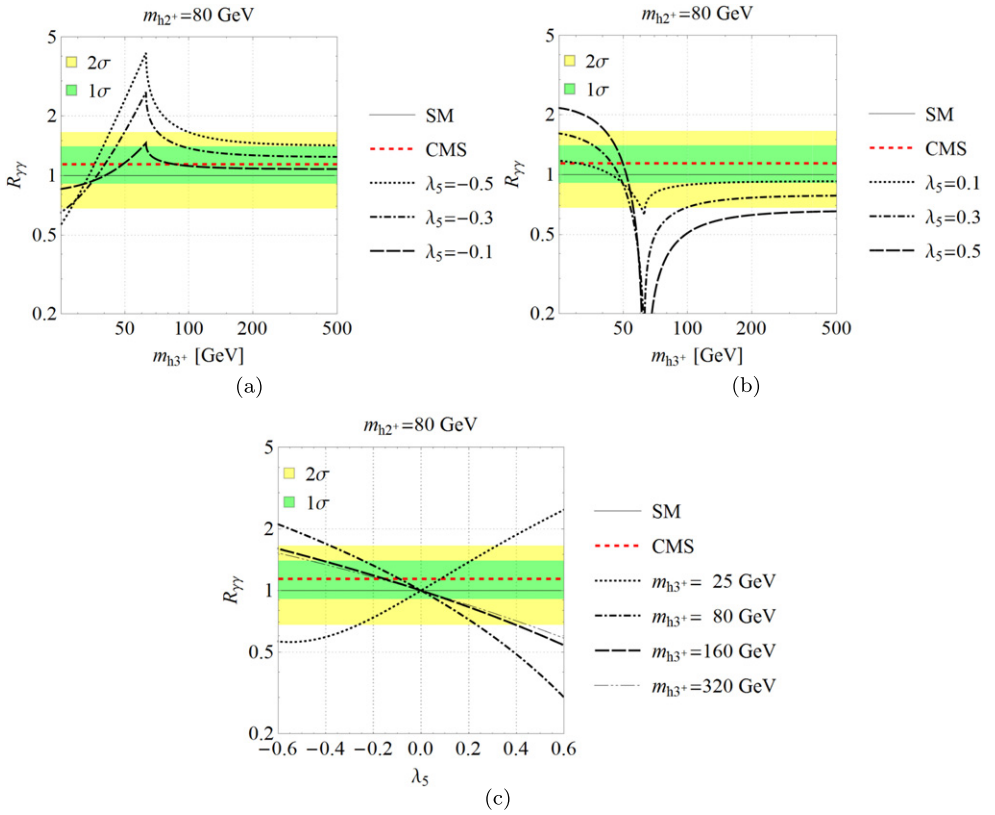

Figure 3. $R_{\gamma\gamma}$ with $m_{h_2^+} = 80$ GeV. In (a) and (b) $R_{\gamma\gamma}$ is a function of $m_{h_3^+} \geqslant 25$ GeV, but in (a) λ_5 is negative and in (b) it is positive. In (c) $R_{\gamma\gamma}$ is presented as a function of $-0.6 \leqslant \lambda_5 \leqslant 0.6$ with different values of $m_{h_3^+}$.

than the SM prediction—see table 1. In figure 4 we illustrate the $R_{\gamma Z}$ results; this decay has almost the same shape and behavior as the two photons channel, except that now the signal is more suppressed when considering the same parameters λ_5 and $m_{h_{2,3}^+}$. This result is congruent because $h \to \gamma\gamma$ has massless particles in the final state, while $h \to \gamma Z$ produces one heavy particle; therefore it is expected that the latter process wibe less sensitive to the common parameters. Therefore, in our results, all analysis applied to $h \to \gamma\gamma$ also applies analogously to $h \to \gamma Z$, where the scenario of negative λ_5 and $m_{h_{2,3}^+} > 80$ GeV agrees mostly with the more accurate experimental data for the two photons channel.

In order to accurately test our parameters, we make a direct comparison of our $R_{\gamma\gamma}$ with the CMS data, namely, $R_{\gamma\gamma}\left(\lambda_5, m_{h_{2,3}^+}\right) = R_{\gamma\gamma}^{\text{CMS}} = 1.14^{+0.26}_{-0.23}$; for this we seek the values for which λ_5 and $m_{h_{2,3}^+}$ satisfy the experimental central value and also $\pm 1\sigma$ deviations around it, where $+1\sigma = 0.26$ and $-1\sigma = 0.23$. When considering -1σ, then $R_{\gamma\gamma}$ falls to 0.91, and for $+1\sigma$ it reaches 1.40. In figure 5(a) with $m_{h_2^+} = 80$ GeV, within $-0.6 \leqslant \lambda_5 \leqslant 0.6$ and $m_{h_3^+} \geqslant m_{h_2^+}$ the curves show the set of parameter values that meet the expectations for $R_{\gamma\gamma}^{\text{CMS}}$; we have also considered some sigma deviations in order to test our parameters; in figure 5(b) the case $m_{h_2^+} = 160$ GeV is presented, and in (c) $m_{h_2^+} = 320$ GeV.

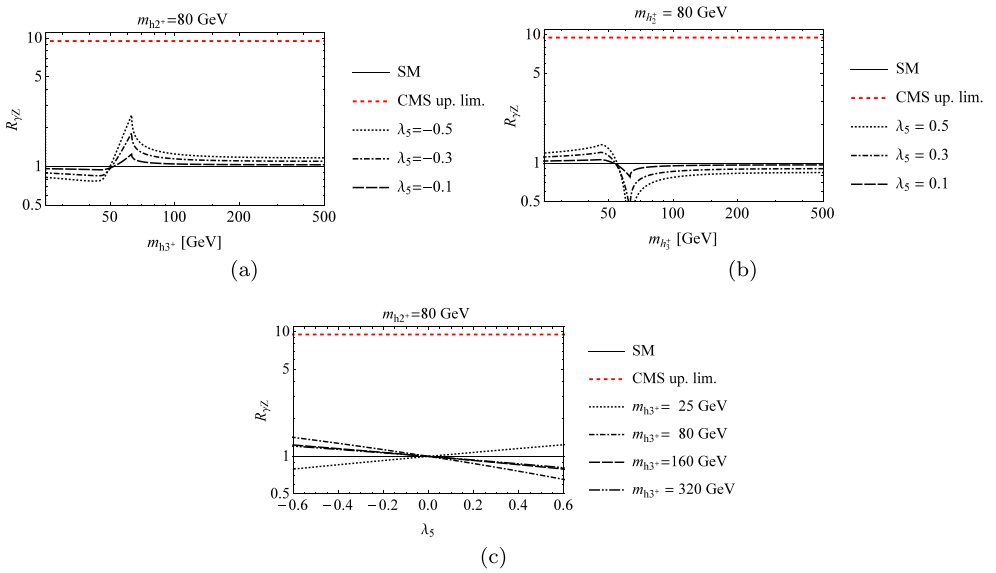

Figure 4. $R_{\gamma Z}$ with $m_{h_2^+} = 80$ GeV. In (a) and (b) $R_{\gamma Z}$ is a function of $m_{h_3^+} \geqslant 25$ GeV, but in (a) λ_5 is negative and in (b) it is positive. In (c) $R_{\gamma\gamma}$ is presented as a function of $-0.6 \leqslant \lambda_5 \leqslant 0.6$ with different values of $m_{h_3^+}$.

Regarding the channel $h \to \gamma Z$, we can now predict the $R_{\gamma Z}$ behavior from the $R_{\gamma\gamma}$ graphs given in figure 5 due to the dependence on common parameters. For this we evaluate in $R_{\gamma Z}$ the set of values that trace the curves for $R_{\gamma\gamma}$ in figure 5, and in table 2 we present the predictions for $R_{\gamma Z}$. We have found that for $m_{h_{2,3}^+} \geqslant 80$ GeV and $-0.6 \leqslant \lambda_5 \leqslant 0.6$ there occurs a constant correlation between both channels: with respect to the central value with $m_{h_2^+} = 80$ GeV, our prediction is $R_{\gamma Z} = 1.06$, and with $m_{h_2^+} \geqslant 160$ GeV it is $R_{\gamma Z} = 1.05$; considering -1σ, the suppression is 0.96 and for $+1\sigma$ it rises to 1.16. In table 2 we also report $m_{h_2^+} = 240$ and 400 GeV; although we do not plot them in figure 5, we consider them important for presenting the constant correlated behavior.

4. Conclusions

In this work we have considered the SM-like Higgs scalar decaying in $\gamma\gamma$ and γZ in the context of the IDMS_3 model which are also candidates for DM. Both decays may have ratios $R_{\gamma\gamma}$ and $R_{\gamma Z}$ that can be enhanced or suppressed compared to the values predicted by the SM. The signal of the λ_5 parameter is the most responsible for this positive or negative deviation—see figures 3–5. The shape and behavior of the curves in both processes are very similar, and the difference between them is due to the massive particle in the final state of the $h \to \gamma Z$ channel. Therefore, it is expected that the latter process will be less sensitive than the two photons channel related to the common parameters λ_5 and $m_{h_{2,3}^+}$. The lower value $m_{h_3^+} > 25$ GeV was obtained from the limit established by the $Z \to h_3^+ h_3^-$ invisible decay. Thus, our parameters are safe by considering this limit. We would like to stress that in the present model both charged scalars $h_{2,3}^+$ do not couple to fermions; they are inert, a fact that highly simplifies the study of the impact of such new spin-0 content on the $h \to \gamma\gamma$, γZ processes. Since they do not couple with fermions, the lower limit obtained by LEP and LHC

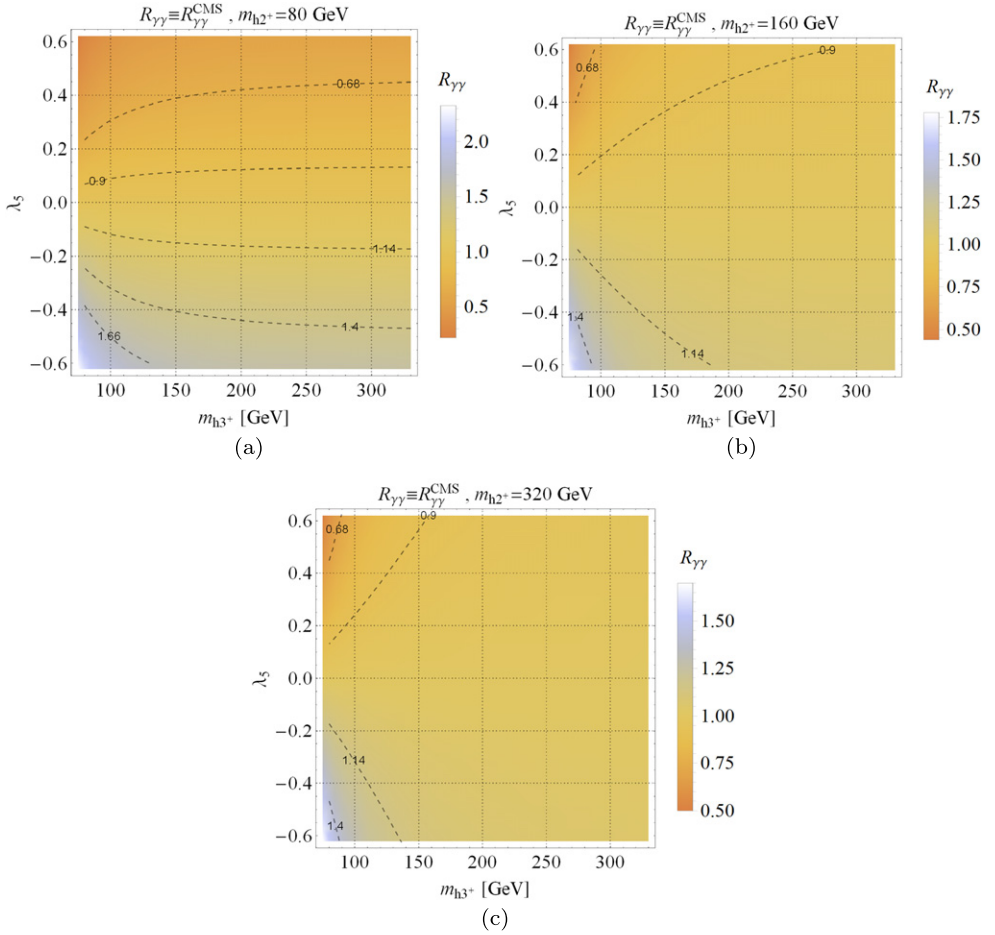

Figure 5. Specific values of $R_{\gamma\gamma} \equiv R_{\gamma\gamma}^{\rm CMS} = 1.14^{+0.26}_{-0.23}$ [6] around the central value considering some σ deviations, with the cases (a) $m_{h_2^+} = 80$ GeV, (b) $m_{h_2^+} = 160$ GeV, and (c) $m_{h_2^+} = 320$ GeV, with $m_{h_3^+} \geqslant 80$ GeV and $-0.6 \leqslant \lambda_5 \leqslant 0.6$.

does not apply in this case. However, for at least one scalar, we use $m_{h_2^+} > 80$ GeV from ATLAS [36].

Following the results from CMS [6] for $R_{\gamma\gamma}$, we have explored the scenarios for the parameters λ_5, $m_{h_2^+}$ and $m_{h_3^+}$ which satisfies specific $R_{\gamma\gamma}$ values considering the experimental sigma deviation. We have concentrated our scenarios within $-0.6 \leqslant \lambda_5 \leqslant 0.6$, $m_{h_2^+} \geqslant 80$ GeV and $m_{h_3^+} \geqslant 25$ GeV. It is worth mentioning that $-0.4 \leqslant \lambda_5 \leqslant 0.4$ is consistent with our results in [11], where we showed reasonable values of this model that can accommodate DM candidates.

Regarding the signal of the λ_5 parameter, we would like to draw attention to a similar analysis that was done in the context of a general three Higgs doublets with S_3 symmetry, but without inert doublets, in [24]. In that case, both decays only have suppressions compared to the SM value: $R_{\gamma\gamma} \in [0.42, 0.80]$ and $R_{\gamma Z} \in [0.73, 0.93]$. The difference between the analysis presented here and the one of [24] is that in our case the μ_d^2 parameter does not

Table 2. Predictions for $R_{\gamma Z}$ from $R_{\gamma\gamma} \equiv R_{\gamma\gamma}^{\mathrm{CMS}} = 1.14^{+0.26}_{-0.23}$ [6] around the central value considering σ deviations, within $-0.6 \leqslant \lambda_5 \leqslant 0.6$, $m_{h_3^+} \geqslant 80$ GeV and with different fixed values from $m_{h_2^+} \geqslant 80$ GeV. The evolution of λ_5 and $m_{h_3^+}$ can be seen explicitly in figure 5 for the cases $m_{h_2^+} = 80$, 160, and 320 GeV. The number absence means prediction out of the λ_5 interval.

Deviation	$R_{\gamma\gamma}$	$R_{\gamma Z}$				
		$m_{h_2^+} = 80$ GeV	$m_{h_2^+} = 160$ GeV	$m_{h_2^+} = 240$ GeV	$m_{h_2^+} = 320$ GeV	$m_{h_2^+} = 400$ GeV
$+2\sigma$	1.66	1.26	—	—	—	—
$+1\sigma$	1.40	1.16	1.16	1.16	1.16	1.16
$0\ \sigma$	1.14	1.06	1.05	1.05	1.05	1.05
-1σ	0.91	0.96	0.96	0.96	0.96	0.96
-2σ	0.68	0.86	0.86	0.86	0.86	0.86

contribute to the spontaneous symmetry breaking. In our analysis, the masses of the scalars are not limited by v_{SM}^2 and by λs of the scalar potentials; this allows positive and negative values for λ_5, whereas in [24] the respective parameter is always negative—see their equation (46). Our analysis is congruent with theirs when our λ_5 is positive. An earlier analysis, also about the parameter space of both ratios in the IDM model, can be found in [22].

In our IDMS_3 a constant correlation occurs between the two processes when considering the scenario $m_{h_{2,3}^+} \geqslant 80$ GeV and $-0.6 \leqslant \lambda_5 \leqslant 0.6$; this fact enables us to predict $R_{\gamma Z}$ from a given $R_{\gamma\gamma}$. Therefore, the comparison of our $R_{\gamma\gamma}$ with the $R_{\gamma\gamma}^{\mathrm{CMS}} = 1.14^{+0.26}_{-0.23}$ allows us to make such predictions—they are given in table 2: with respect to the central value when considering $m_{h_2^+} = 80$ GeV, our prediction is $R_{\gamma Z} = 1.06$; and when $m_{h_2^+} \geqslant 160$ GeV, our prediction is $R_{\gamma Z} = 1.05$; in addition, for $m_{h_2^+} \geqslant 80$, GeV considering $+1\sigma$, the ratio reaches 1.16, while for -1σ it yields 0.96. This kind of behavior has been observed in other multi-Higgs models that include real [37] or complex [38] triplets, so this seems to be a general feature of multi-Higgs models.

Otherwise, the experimental reports on the $h \to \gamma Z$ decay will continue offering upper limits of one order of magnitude greater than the SM prediction, as commented on the Introduction, and it is expected that at LHC Run 6 [25, 26] it will reach a luminosity of 3000 fb^{-1} of pp collisions; we could then measure this mode with a precision of 54%–57% at ATLAS and of 20%–24% at CMS. What if an important increment is detected in future reports? One possible answer to this question could be that maybe this is due to new physics effects that possible require a different coupling of the new particle with the Z boson. For sure, it will be an invitation to revisit the status of the SM. In the SM, the decay $h \to \gamma Z$ is essentially due to the virtual W gauge boson contribution, and the destructive interference caused by the top quark is not very significant; therefore the search of a deviation in this process is unlikely due to a possible correction in the $Zf\bar{f}$ vertices and besides the decay $Z \to f\bar{f}$ is well known.

Acknowledgments

ACBM thanks CAPES for financial support. ECFSF and JM thank FAPESP for financial support under the respective processes number 2011/21945-8 and 2013/09173-5. VP thanks CNPq for partial support. JM is grateful to Daniel Alva for useful discussions.

Appendix. Form factors and the Passarino–Veltman scalar functions

Here we present explicitly the form factors A_{Spin} [32, 33], given in equations (13) and (15), in terms of the B_0 and C_0 Passarino–Veltman scalar functions [30]. We have constructed and solved each loop diagram with the Passarino–Veltman reduction method [28] using `FeynCalc` [29], and also obtained the corresponding analytical solutions for the B_0 and C_0 scalar integrals via the Feynman parametrization method and dimensional regularization scheme [28, 39–41]. The solutions have been verified numerically using `LoopTools` [42]. We have refrained from showing the construction of the loop integrals of the processes because they are frequently presented in the literature; instead we write down in detail the final result of the tensorial amplitudes, since they are usually omitted in terms of the Passarino–Veltman functions and even more unknown are their general analytical solutions, which we found more practical for numerical evaluation, that is, without the need of splitting them in cases.

The one-loop decay $h \to \gamma\gamma$ is a low order process; therefore it is ultraviolet (UV) finite as there is no tree-level $h\gamma\gamma$ coupling in the Lagrangian, since the SM is a renormalizable theory, hence counterterms $h\gamma\gamma$ cannot be present. The same argument applies to $h \to \gamma Z$ in the absence of $h\gamma Z$ interaction.

For the $h \to \gamma\gamma$ decay, with configuration $h(p_3) \to \gamma_{\mu_1}(p_1)\gamma_{\mu_2}(p_2)$, the amplitude is

$$\mathcal{M}_{h\to\gamma\gamma} = \mathcal{M}^{\mu_1\mu_2}_{\gamma\gamma}\epsilon^*_{\mu_1}(\vec{p}_1,\,\lambda_1)\epsilon^*_{\mu_2}(\vec{p}_2,\,\lambda_2), \tag{A1}$$

with kinematics $p_3 = p_1 + p_2$, $p_3^2 = m_h^2$, $p_1^2 = p_2^2 = 0$, $p_1 \cdot p_2 = m_h^2/2$, and transversality conditions $p_1 \cdot \epsilon^*(\vec{p}_1,\,\lambda_1) = p_2 \cdot \epsilon^*(\vec{p}_2,\,\lambda_2) = 0$. The tensorial amplitude is

$$\begin{aligned}\mathcal{M}^{\mu_1\mu_2}_{\gamma\gamma} = &-i\frac{\sqrt{\sqrt{2}\,G_F}}{2\pi}\,\alpha\left[\sum_{i=1}^{9}N_C^{f_i}Q_{f_i}^2A^{\gamma\gamma}_{1/2}(\tau_{f_i}) + A_1^{\gamma\gamma}(\tau_W) + \frac{\lambda_5 v_{\text{SM}}^2}{2}\sum_{i=2}^{3}\frac{1}{m^2_{h_i^+}}A_0^{\gamma\gamma}(\tau_{h_i^+})\right]\\ &\times\left(\frac{m_h^2}{2}g^{\mu_1\mu_2} - p_2^{\mu_1}p_1^{\mu_2}\right),\end{aligned} \tag{A2}$$

where $\tau_X \equiv m_h^2/4m_X^2$ and $X = f,\, W,\, h^\pm$, which satisfies electromagnetic gauge invariance via the accomplishment of the Ward identities $p_{1\mu_1}\mathcal{M}^{\mu_1\mu_2}_{\gamma\gamma} = p_{2\mu_1}\mathcal{M}^{\mu_1\mu_2}_{\gamma\gamma} = 0$. The form factors are

$$\begin{aligned}A^{\gamma\gamma}_{1/2} &\equiv \frac{4m_f^2}{m_h^2}\left[2 + \left(4m_f^2 - m_h^2\right)C_0^{h,f}\right]\\ &= 2\left[\tau_f + \left(\tau_f - 1\right)f(\tau_f)\right]\tau_f^{-2},\end{aligned} \tag{A3}$$

$$\begin{aligned}A_1^{\gamma\gamma} &\equiv -2\left\{1 + 6\frac{m_W^2}{m_h^2}\left[1 + \left(2m_W^2 - m_h^2\right)C_0^{h,W}\right]\right\}\\ &= -\left[2\tau_W^2 + 3\tau_W + 3\left(2\tau_W - 1\right)f(\tau_W)\right]\tau_W^{-2},\end{aligned} \tag{A4}$$

$$A_0^{\gamma\gamma} \equiv -\frac{4m_{h^+}^2}{m_h^2}\Big(1 + 2m_{h^+}^2 C_0^{h,h^+}\Big)$$
$$= -\Big[\tau_{h^+} - f(\tau_{h^+})\Big]\tau_{h^+}^{-2}, \tag{A5}$$

$$f(\tau) \equiv \begin{cases} \arcsin^2\sqrt{\tau}, & \tau \leqslant 1 \\ -\frac{1}{4}\left(\log\frac{1+\sqrt{1-\tau^{-1}}}{1-\sqrt{1-\tau^{-1}}} - i\pi\right)^2, & \tau > 1 \end{cases}, \quad \tau \equiv \frac{m_h^2}{4m_X^2}. \tag{A6}$$

The three-point Passarino–Veltman scalar function is

$$C_0^{h,X} \equiv C_0\Big(0,\, 0,\, m_h^2,\, m_X^2,\, m_X^2,\, m_X^2\Big)$$
$$= \frac{1}{2m_h^2}\log^2\left(-\frac{1+\sqrt{1-\frac{4\left(m_X^2-i\epsilon\right)}{m_h^2}}}{1-\sqrt{1-\frac{4\left(m_X^2-i\epsilon\right)}{m_h^2}}}\right)$$
$$= -\frac{2}{m_h^2}\arctan^2\frac{-i}{\sqrt{1-\frac{4\left(m_X^2-i\epsilon\right)}{m_h^2}}}$$
$$= -\frac{2}{m_h^2}f(\tau). \tag{A7}$$

For the $h \to \gamma Z$ decay, with configuration $h(p_3) \to \gamma_{\mu_1}(p_1) Z_{\mu_2}(p_2)$, the amplitude is

$$\mathcal{M}_{\gamma Z} = \mathcal{M}_{\gamma Z}^{\mu_1\mu_2}\epsilon_{\mu_1}^*\big(\vec{p}_1,\, \lambda_1\big)\epsilon_{\mu_2}^*\big(\vec{p}_2,\, \lambda_2\big), \tag{A8}$$

with kinematics $p_3 = p_1 + p_2$, $p_3^2 = m_h^2$, $p_1^2 = 0$, $p_2^2 = m_Z^2$, $p_1 \cdot p_2 = (m_h^2 - m_Z^2)/2$, and transversality conditions $p_1 \cdot \epsilon^*(\vec{p}_1,\, \lambda_1) = p_2 \cdot \epsilon^*(\vec{p}_2,\, \lambda_2) = 0$. The tensorial amplitude is

$$\mathcal{M}_{h\to\gamma Z}^{\mu_1\mu_2} = i\frac{\sqrt{\alpha}G_F m_W}{\sqrt{2}\,\pi^{3/2}}\Bigg[\frac{2}{c_W}\sum_{i=1}^{9}N_C^{f_i}Q_{f_i}g_V^{f_i}A_{1/2}^{\gamma Z}(\tau_{f_i}) + A_1^{\gamma Z}(\tau_W)$$
$$+ \frac{\lambda_5 v_{\rm SM}^2 v_{h^\pm}}{2}\sum_{i=2}^{3}\frac{1}{m_{h_i^+}^2}A_0^{\gamma Z}(\tau_{h_i^+})\Bigg],$$
$$\times\left(\frac{m_h^2 - m_Z^2}{2}g^{\mu_1\mu_2} - p_2^{\mu_1}p_1^{\mu_2}\right), \tag{A9}$$

where $\tau_X \equiv 4m_X^2/m_h^2$, $\lambda_X \equiv 4m_X^2/m_Z^2$ and $X = f,\, W,\, h^\pm$, which satisfies $U(1)_{\rm em}$ gauge invariance through the fulfilment of the Ward identity for the photon $p_{1\mu_1}\mathcal{M}_{\gamma Z}^{\mu_1\mu_2} = 0$. Moreover, in this process the Ward identity for the Z boson $p_{2\mu_1}\mathcal{M}_{\gamma Z}^{\mu_1\mu_2} = 0$ is also satisfied. The form factors are

$$A_{1/2}^{\gamma Z} = -\frac{2m_f^2}{m_h^2 - m_Z^2} - \frac{2m_Z^2 m_f^2}{\left(m_h^2 - m_Z^2\right)^2}\Big(B_0^{h,f} - B_0^{Z,f}\Big) + m_f^2\left(1 - \frac{4m_f^2}{m_h^2 - m_Z^2}\right)C_0^{h,Z,f}$$
$$= I_1\big(\tau_f,\, \lambda_f\big) - I_2\big(\tau_f,\, \lambda_f\big), \tag{A10}$$

$$A_1^{\gamma Z} = \frac{1}{m_W m_Z\left(m_h^2 - m_Z^2\right)^2}\Big\{\Big[2m_W^2\left(m_h^2 + 6m_W^2\right) - m_Z^2\left(m_h^2 + 2m_W^2\right)\Big] \times\Big[m_h^2 - m_Z^2 + m_Z^2\left(B_0^{h,W} - B_0^{Z,W}\right)\Big] + 2\left(m_h^2 - m_Z^2\right)m_W^2\Big[6m_W^2\left(2m_W^2 + m_Z^2\right) - 2m_Z^4 + m_h^2\left(m_Z^2 - 6m_W^2\right)\Big]C_0^{h,Z,W}\Big\} = c_W\Big\{4\left(3 - t_W^2\right)I_2(\tau_W, \lambda_W) + \Big[\left(1 + 2\tau_W^{-1}\right)t_W^2 - \left(5 + 2\tau_W^{-1}\right)\Big]I_1(\tau_W, \lambda_W)\Big\}, \tag{A11}$$

$$A_0^{\gamma Z} = \frac{2m_{h^+}^2}{\left(m_h^2 - m_Z^2\right)^2}\Big[m_Z^2\left(B_0^{h,h^+} - B_0^{Z,h^+}\right) + \left(m_h^2 - m_Z^2\right)\left(1 + 2m_{h^+}^2 C_0^{h,Z,h^+}\right)\Big] = -I_1\left(\tau_{h^+}, \lambda_{h^+}\right), \tag{A12}$$

and the auxiliary functions

$$I_1(\tau, \lambda) \equiv \frac{\tau\lambda}{2(\tau - \lambda)} + \frac{\tau^2\lambda^2}{2(\tau - \lambda)^2}\Big[f\left(\tau^{-1}\right) - f\left(\lambda^{-1}\right)\Big] + \frac{\tau^2\lambda}{(\tau - \lambda)^2}\Big[g\left(\tau^{-1}\right) - g\left(\lambda^{-1}\right)\Big],$$
$$I_2(\tau, \lambda) \equiv -\frac{\tau\lambda}{2(\tau - \lambda)}\Big[f\left(\tau^{-1}\right) - f\left(\lambda^{-1}\right)\Big]. \tag{A13}$$

We emphasize that here in $h \to \gamma Z$, $\tau \equiv 4m_X^2/m_h^2$ is used, opposite to the $h \to \gamma\gamma$ case; therefore here $f(\tau^{-1})$ evaluates $\tau^{-1} = m_h^2/4m_X^2$ for consistency because originally $f(\tau)$ is defined in equation (A6) with $\tau \equiv m_h^2/4m_X^2$. Exactly the same situation holds for

$$g(\tau) \equiv \begin{cases} \sqrt{\tau^{-1} - 1}\arcsin\sqrt{\tau}, & \tau \leqslant 1 \\ \frac{\sqrt{1-\tau^{-1}}}{2}\left(\log\frac{1 + \sqrt{1-\tau^{-1}}}{1 - \sqrt{1-\tau^{-1}}} - i\pi\right), & \tau > 1 \end{cases}, \ \tau \equiv \frac{m_h^2}{4m_X^2}, \tag{A14}$$

where we disagree with the inequalities orientations given in [32, 33], but the correct definition can be found in the same author's [34], as also used in [20].

The two-point scalar function, with its UV divergent term Δ, is

$$B_0^{h,X} = B_0\left(m_h^2, m_X^2, m_X^2\right) = \Delta - \log\frac{m_X^2}{\mu^2} + 2 - \sqrt{1 - \frac{4\left(m_X^2 - i\epsilon\right)}{m_h^2}}\log\left(-\frac{1 + \sqrt{1 - \frac{4\left(m_X^2 - i\epsilon\right)}{m_h^2}}}{1 - \sqrt{1 - \frac{4\left(m_X^2 - i\epsilon\right)}{m_h^2}}}\right)$$
$$= \Delta - \log\frac{m_X^2}{\mu^2} + 2 - 2\,i\sqrt{1 - \frac{4\left(m_X^2 - i\epsilon\right)}{m_h^2}}\arctan\frac{-i}{\sqrt{1 - \frac{4\left(m_X^2 - i\epsilon\right)}{m_h^2}}}$$
$$= \Delta - \log\frac{m_X^2}{\mu^2} + 2 - 2\ g(\tau), \tag{A15}$$

$$\Delta \equiv \frac{2}{4 - D} - \gamma_E + \log 4\pi, \tag{A16}$$

where $g(\tau)$ is in accordance with equation (A14), and the difference of two B_0 with the same virtual masses yields the UV-finite result

$$B_0^{h,X} - B_0^{Z,X} = -2[g(\tau) - g(\lambda)]. \tag{A17}$$

The `LoopTools` program evaluates any B_0 without the $\Delta + \log \mu^2$ term by default because in any UV-finite process such terms must vanish, e.g. equation (A17).

Finally, the last three-point scalar function is

$$\begin{aligned} C_0^{h,Z,X} &\equiv C_0\left(0, m_h^2, m_Z^2, m_X^2, m_X^2, m_X^2\right) \\ &= \frac{m_h^2 C_0^{h,X} - m_Z^2 C_0^{Z,X}}{m_h^2 - m_Z^2} \\ &= \frac{-2}{m_h^2 - m_Z^2}[f(\tau) - f(\lambda)], \end{aligned} \tag{A18}$$

where $C_0^{h,X}$ and $C_0^{Z,X}$ are given in equation (A7).

References

[1] Aad G *et al* (ATLAS Collaboration) 2013 *Phys. Lett.* B **726** 120
Aad G *et al* (ATLAS Collaboration) ATLAS-CONF-2013-040
[2] Chatrchyan S *et al* (CMS Collaboration) 2013 *Phys. Rev. Lett.* **110** 081803
[3] Aad G *et al* (ATLAS Collaboration) 2012 *Phys. Lett.* B **716** 1
[4] Chatrchyan S *et al* (CMS Collaboration) 2012 *Phys. Lett.* B **716** 30
[5] Aad G *et al* (ATLAS Collaboration) 2014 The ATLAS detector *Phys. Rev.* D **90** 112015
[6] Khachatryan V *et al* (CMS Collaboration) 2014 *Eur. Phys. J.* C **74** 3076
[7] Aad G *et al* (ATLAS Collaboration) 2014 *Phys. Lett.* B **732** 8
[8] Chatrchyan S *et al* (CMS Collaboration) 2013 *Phys. Lett.* B **726** 587
[9] Machado A C B and Pleitez V 2012 (arXiv:1205.0995)
[10] Cardenas H, Machado A C B, Pleitez V and Rodriguez J-A 2013 *Phys. Rev.* D **87** 035028
[11] Fortes E C F S, Machado A C B, Montaño J and Pleitez V 2014 (arXiv:1407.4749)
[12] Lopez Honorez L, Nezri E, Oliver J F and Tytgat M H G 2007 *J. Cosmol. Astropart. Phys.* JCAP02(2007)028
[13] Hambye T and Tytgat M H G 2008 *Phys. Lett.* B **659** 651
[14] Dolle E, Miao X, Su S and Thomas B 2010 *Phys. Rev.* D **81** 035003
[15] Lopez Honorez L and Yaguna C E 2011 *J. Cosmol. Astropart. Phys.* JCAP01(2011)002
[16] Gustafsson M, Rydbeck S, Lopez-Honorez S and Lundstrom E 2012 *Phys. Rev.* D **86** 075019
[17] Goudelis A, Herrmann B and Stål O 2013 *J. High Energy Phys.* JHEP09(2013)106
[18] Cao Q-H, Ma E and Rajasekaran G 2007 *Phys. Rev.* D **76** 095011
[19] Lundstrom E, Gustafsson M and Edsjo J 2009 *Phys. Rev.* D **79** 035013
[20] Swiezewska B and Krawczyk M 2013 *Phys. Rev.* D **88** 035019
[21] Barbieri R, Hall L J and Rychkov V S 2006 *Phys. Rev.* D **74** 015007
[22] Krawczyk M, Sokołowska D, Swaczyna P and Świeżewska B 2013 *Acta Phys. Polon.* B **44** 2163
[23] Chen C-S, Geng C-Q, Huang D and Tsai L-H 2013 *Phys. Rev.* D **87** 075019
[24] Das D and Dey U K 2014 *Phys. Rev.* D **89** 095025
[25] Dawson S *et al* 2013 (arXiv:1310.8361)
[26] Krohan H 2014 ATL-PHYS-SLIDE-2014-033 (https://cds.cern.ch/record/1645635)
Okawa H 2014 ATL-PHYS-SLIDE-2014-211 (https://cds.cern.ch/record/1702705?ln=sv)
Canepa A 2015 ATL-PHYS-SLIDE-2015-011 (https://cdsweb.cern.ch/record/1984417?ln=pt)
[27] Ishimori H, Kobayashi T, Ohki H, Shimizu Y, Okada H and Tanimoto M 2010 *Prog. Theor. Phys. Suppl.* **183** 1
[28] Passarino G and Veltman M J G 1979 *Nucl. Phys.* B **160** 151
[29] Mertig R, Bohm M and Denner A 1991 *Comput. Phys. Commun.* **64** 345
[30] 't Hooft G and Veltman M J G 1979 *Nucl. Phys.* B **153** 365
[31] Gunion J F, Haber H E, Kane G L and Dawson S 2000 *Front. Phys.* **80** 1

[32] Djouadi A 2008 *Phys. Rep.* **457** 1
[33] Djouadi A 2008 *Phys. Rep.* **459** 1
[34] Spira M, Djouadi A, Graudenz D and Zerwas P M 1995 *Nucl. Phys.* B **453** 17
[35] Abbiendi G *et al* [ALEPH and DELPHI and L3 and OPAL and LEP Collaborations] 2013 *Eur. Phys. J.* C **73** 2463
[36] Aad G *et al* (ATLAS Collaboration) 2013 *Eur. Phys. J.* C **73** 2465
[37] Arina C, Martin-Lozano V and Nardini G 2014 *J. High Energy Phys.* JHEP08(2014)015
[38] Chen C H and Nomura T 2014 *J. High Energy Phys.* JHEP09(2014)120
[39] Peskin M E and Schroeder D V 1995 *An Introduction to Quantum Field Theory* (Reading, MA: Addison-Wesley) p842
[40] Bardin D Y and Passarino G 1999 *The Standard Model in the Making: Precision Study of the Electroweak Interactions* (*International Series of Monographs on Physics 40*) (Oxford: Oxford University Press)
[41] Bohm M, Denner A and Joos H 2001 *Gauge Theories of the Strong and Electroweak Interaction* (Leipzig: Teubner) p 784
[42] Hahn T and Perez-Victoria M 1999 *Comput. Phys. Commun.* **118** 153